

Fast Marching based Rendezvous Path Planning for a Team of Heterogeneous Vehicle

Jaekwang Kim¹, Hyung-Jun Park², Jaejeong Shin^{3,*}

¹*Department of Mechanical and Design Engineering, Hongik University, Republic of Korea*

²*Platform Technology Research Center, Corporate R&D, LG Chem*

³*Department of Mechanical and Aerospace Engineering, University of Florida*

jk12@hongik.ac.kr, constlearner89@gmail.com, jane.shin@ufl.edu

* Corresponding author

Abstract

A formulation is developed for deterministically calculating the optimized paths for a multi-agent system consisting of heterogeneous vehicles. The essence of this formulation is the calculation of the shortest time for each agent to reach every grid point from its known initial position. Such arrival time map can be readily assessed using the Fast Marching Method (FMM), a computational algorithm originally designed for solving boundary value problems of the Eikonal equation. Leveraging the FMM method, we demonstrate that the minimal time rendezvous point and paths for all member vehicles can be uniquely determined with minimal computational concerns. To showcase the potential of our method, we use an example of a virtual rendezvous scenario that entails the coordination of a ship, an underwater vehicle, an aerial vehicle, and a ground vehicle to converge at the optimal location within the Tampa Bay area in minimal time. It illustrates the value of the developed framework in efficiently constructing continuous path planning, while accommodating different operational constraints of heterogeneous member vehicles.

Keywords— Fast marching method, Path planning, Heterogeneous vehicles, Multi-agent system, Autonomous Vehicles

1 Introduction

Recent advancements in various types of autonomous vehicles have sparked interest in multi-agent systems, which hold the potential to efficiently address complex tasks. Strategic multi-agent path finding (MAPF) becomes crucial, particularly when the team comprises heterogeneous vehicles with varying operational domains and capabilities, such as different speeds, sizes, and maneuverability. These agents may encompass a wide range of vehicles, including ships, underwater vehicles, aerial vehicles, and ground vehicles. Each type of vehicle can have unique navigational constraints and environmental interactions [1, 2]. Previous studies in multi-agent planning have primarily concentrated on scheduling, with an emphasis on task allocation and agent coordination [3]. However, these approaches have warranted a rigorous continuous path ¹ planning that ensures smooth and uninterrupted motion of vehicles [4], since all agents in real-world applications must adapt their paths in response to changing environmental conditions and dynamic obstacles.

¹Here, a continuous path refers to a path defined on continuous real-world space and thus can serve as a smooth path for autonomous vehicles.

In the perspective of computational science, a general form of continuous MAPF is known as an NP-hard problem [5]. One of the main challenges is related to the high dimensionality of the problem. With many agents in an environment, the number of potential paths and interactions can become overwhelmingly large. The complexity of the multi-agent path finding problem also stiffly increases, as the problem as the number of agents in the system increases, and thus solving MAPF problems becomes computationally expensive. Moreover, in many cases, efficiency is not the sole concern; safety (collision-free paths) must also be taken into account. Due to the complex nature and conflicting objectives encountered in MAPF problems, in many cases, one needs to reduce or approximate the original problem to a simpler form, compromising accuracy and global optimality.

In this work, we consider continuous path planning of a multi-agent system for minimal time rendezvous tasks. In these tasks, some agents initially operating at different locations are tasked with meeting to exchange information or resources. Such type of tasks are frequently encountered in spacecraft docking scenarios [6, 7]. A team of autonomous underwater vehicles also often needs to initiate information exchange tasks at close distances due to limited data transfer capabilities in deep water [8]. In these scenarios, identifying the optimal rendezvous point and the path for each agent to achieve the earliest possible rendezvous time as a team (or other optimizing goals) is important. Unfortunately, however, planning paths that accommodate differences of vehicles, while optimizing overall performance remains a significant challenge.

The primary contribution of this paper lies in formulating the rendezvous problem of a multi-agent system in a way that is suitable for assessment using the fast marching method (FMM). The FMM is a well-established numerical technique originally developed for solving the Eikonal equation. Beyond its original purpose, however, the FMM has also demonstrated its capability in efficiently computing the shortest paths on continuous grids [9, 10, 11, 12, 13]. Extending these works, we show how the use of the FMM for rendezvous MAPF also enables the enhancement of collaboration, reduction of complexity, and optimization of the overall mission performance of the team. Specifically, we first define an optimization problem that involves continuous path planning for a team of heterogeneous vehicles, each with its operational domain. Then, we exploit the direct output from the FMM as a key component of a new path planning approach. Our approach deterministically calculates the time-optimal rendezvous point for heterogeneous vehicles and determines the path to the optimal rendezvous point from different initial agent positions. Throughout this process, the method also takes into account their unique operational constraints and environmental interactions.

The remainder of the paper is organized as follows. Section 2 introduces methodologies of the FMM and FMM-based path planning. In Section 3, we formulate an optimization problem for multi-agent path planning of a rendezvous task and introduce a new methodology based on to efficiently solve the problem. Section 4 presents a virtual path planning experiment to demonstrate the potential of our proposed approach, while Section 5 discusses important features and highlights merits of the suggested methodology. Finally, we conclude the paper in Section 6, listing potential future research directions.

2 Background on Fast Marching Method and Its Application to Path Optimization

In this section, we provide a brief overview of the FMM, which will be used to address the challenges of multi-agent path planning for rendezvous missions. Originally developed for solving a nonlinear first-order partial differential equation, the FMM has shown high efficiency in dealing with interface mechanics compared to other algorithms [14, 15, 16, 17]. The FMM has also found applications in diverse research domains,

encompassing materials science [18], computer graphics [19], and image processing [20]. Particularly, its application to path optimization has a long history in various domains of applications, ranging from marine vehicles to social navigation [21, 22, 23, 24, 25, 26]. In the following, we begin by summarizing the main ideas of the FMM in its original context.

2.1 The fast marching method

First introduced in Ref. [27], the FMM is an efficient computational algorithm for tracking the front, or *interface*, that evolves with the outward unit normal direction with speed V . The explicit outcome of FMM is the arrival time $T(\mathbf{x})$ that the initial surface needs to reach every point \mathbf{x} on the given domain Ω . For example, Fig. 1 demonstrates the result of FMM used to track an initial surface Γ (the innermost blue line) growing with a uniform outward normal velocity $V(\mathbf{x}) = 1$. In the following, we brief the FMM algorithm as described in Ref. [28].

Let $s(t)$ describe a surface evolving speed $V(\mathbf{x})$ from a given initial surface $s(0) = \Gamma$. Instead of solving a time-dependent problem for $s(t)$ to track the moving surface, the FMM solves a function $T(\mathbf{x})$ defined as

$$T(s(t)) = t, \quad (1)$$

with $T = 0$ on Γ .

Differentiating (1) and noting that ∇T is normal to the surface, one arrives at the following boundary value problem,

$$|\nabla T|V = 1. \quad (2)$$

Also, the boundary condition for T equivalent to the original time-dependent problem is

$$T = 0 \quad \text{on } \Gamma. \quad (3)$$

Equation (2) is commonly referred to as the Eikonal equation.

Now, we describe the algorithm to solve (2) on a two-dimensional discrete grid, i.e. $\mathbf{x} = (x, y)$. However, it is worth noting that the algorithm are conveniently generalized to arbitrary dimensions. Let $D_{ij}^{-x}(\cdot)$ denotes the standard backward-difference operation on the grid point ij

$$D_{ij}^{-x}T = \frac{T_{ij} - T_{(i-1)j}}{\delta x}. \quad (4)$$

Likewise, we use D^{+x} , D^{-y} , and D^{+y} to represent forward in x , backward and forward in y backward finite difference operators, respectively. In order to ensure a unique *viscosity solution* for the eikonal equation (2), we necessitate the consistent utilization of an upwind finite difference scheme when computing the gradient. This is compactly written as

$$\frac{1}{V(\mathbf{x})} = [(\max(D_{ij}^{-x}T, D^{+x}T_{ij}, 0))^2 + \max(D_{ij}^{-y}T, -D^{+y}T_{ij}, 0)^2]^{1/2}. \quad (5)$$

When the neighboring values of T_{ij} are known, the discrete eikonal equation (5) becomes a quadratic equation for T_{ij} at each grid point, allowing for straightforward analytical solutions.

The FMM initiates by performing the following initialization step.

1. Assign $T(\mathbf{x}) = 0$ for grid points in the area enclosed by the initial surface, and tag them as *accepted*
2. Assign $T(\mathbf{x}) = +\infty$ for the remaining grid points, and tag them as *far*
3. Among the *accepted* points, identify the points that are in the neighborhood of points tagged as *far*, and tag them as *considered*

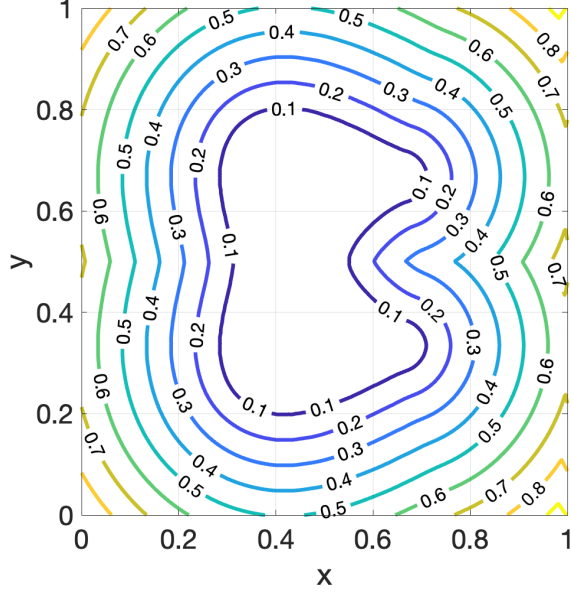


Figure 1: The level sets of the solution to the Eikonal equation (2) computed using the fast marching method, describe a surface evolving with outward normal velocity $V(\mathbf{x}) = 1$. The level set values are indicative of the time it takes for the initial surface (represented by the innermost blue line) to reach each grid point within the computational domain.

The key step in the fast marching method is to update T with a trial value using Eq. (5) for grid points tagged as *considered*, while only accepting the update with the smallest value at each iteration. This procedure requires keeping track of the smallest T -value among points tagged as *considered*. The potential T values are managed in a specialized data structure inspired by discrete network algorithms [29]. This data structure is known as a min-heap data structure, which represents a complete binary tree with a property that the value at any given node is less than or equal to the values of its children. Utilizing the min-heap, the FMM then proceeds as follows.

1. Form a min-heap structure for the *considered* points.
2. Access the minimum value of the heap, located at the root of the binary tree.
3. Determine a trial solution \tilde{T} on the neighbors of the root using Eq. (5). If the trial solution \tilde{T} is smaller than the present values, then update $T(\mathbf{x}) = \tilde{T}$.
4. If a point, previously tagged as *far*, is updated using a trial value, relabel it as *considered*, and add it to the heap structure.
5. Tag the root of the heap as *accepted*, and delete it from the heap.
6. Repeat steps 2 to 5, until every grid point is tagged as *accepted*.

The primal computational complexity of the FMM arises from maintaining the heap structure, which is known to be $\mathcal{O}(n \log n)$, where n is the number of total grid points.

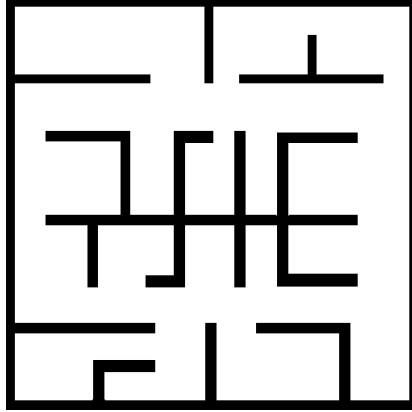


Figure 2: An example of binary occupancy map. The binary image, which is on 512×512 pixel size, takes the value of 0 if the position is occupied by obstacles, and 1 otherwise.

2.2 Adaptation of the FMM for path optimization

While the FMM is originally developed for interface problems, numerous studies have also successfully applied the FMM in vehicle path planning scenarios, enabling agents to navigate complex environments, avoid obstacles, and reach their destinations efficiently. These studies have primarily focused on single-agent path planning under various external conditions. These include time-varying environmental factors, such as waves and currents in oceans [9], time-varying environments with predictive models [10], angle guidance for uncrewed surface vehicles [30], anisotropic Fast Marching (FM)-based approaches for dynamic obstacles [11] and bridge obstacles [12], as well as path planning for autonomous ships [13]. In contrast, its application in multi-agent systems remains relatively unexplored. A few examples include swarm coordination [31] and formation control involving vehicles with different dynamic properties [32].

In the context of path optimization, the computational domain Ω of the FMM takes on a new perspective as the configuration space for mobile agents, often depicted through a binary occupancy map as illustrated in Fig. 2. The binary image, which is in a size of $n = n_1 \times n_2$ pixels, takes the value of 0 if the position is occupied by obstacles, and 1 otherwise. Also, the initial surface Γ is reduced to a single wave-source point \mathbf{x}_0 , representing the initial location of an agent. The velocity field $V(\mathbf{x})$ signifies the permissible speed of vehicles at a given position while considering the proximity of obstacles (such as walls and barriers) to the agents. As part of the FMM’s initialization step, every grid point located on obstacles is initially labeled as “accepted”.

Next, the FMM algorithm is executed to compute the shortest time $T(\mathbf{x})$ for the propagating wave to arrive at each grid point. The trajectory of the agent is finally determined by extracting the maximum gradient direction of $T(\mathbf{x})$ from the target point to the initial point. Since $T(\mathbf{x})$ is derived from the target point, the resulting T -field uniquely exhibits a single minimum at the target point, ensuring a unique solution [23].

A remaining task is to employ an appropriate model for the velocity field $V(\mathbf{x})$ that respects the environment. While one might simply consider the simplest option, which is to use a constant value \mathcal{V}_{max} representing the maximum speed of the agents, it is observed that the resulting trajectory lacks realism as it fails to ensure both smoothness and a safe distance between agents and obstacles [21].

To address these issues, the FMM has been advanced into the Fast Marching Square (FMS) method. In order to guarantee a safe distance between obstacles and agents, this approach introduces a penalty to the agent’s velocity as it navigates in proximity to obstacles. The FMS method entails the implementation of

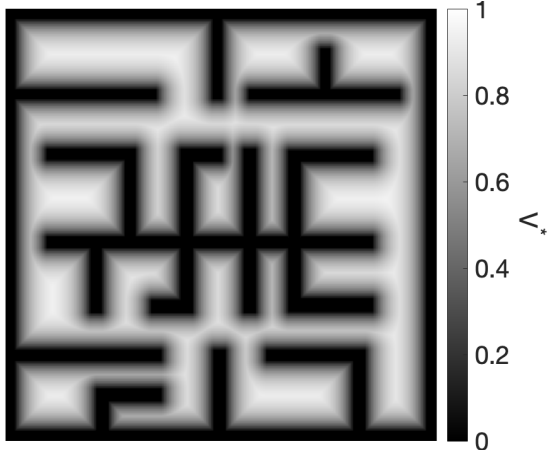


Figure 3: Velocity map created using the form (6) with $\alpha = 3$. The velocity values V^* are normalized with the maximum speed of agent \mathcal{V}_{\max} .

two distinct FMMs.

The objective of the first FMM is to construct a velocity grid map that takes into account the presence of obstacles. This is achieved by evolving initial surfaces, which represent the boundaries of obstacles in the environment, with a constant velocity $V(\mathbf{x}) = 1$. The outcome of this process is the computation of the distance $d(\mathbf{x}) = T(\mathbf{x}) \in \mathbb{R}^+$ at each grid point, indicating the shortest distance to the nearest obstacle. Consequently, a velocity grid map V is computed as a function of d , which is artificially designed to penalize the vehicle's speed as it approaches obstacles. A common choice for this penalizing function is a linear relationship $V \propto d$, which is inspired by a two-dimensional repulsive electrostatic potential [33]. Alternatively, one may also consider

$$V(d(\mathbf{x})) = \mathcal{V}_{\max} \left[1 - \exp \left(-\alpha \left(\frac{d}{d_{\max}} \right) \right) \right], \quad (6)$$

where d_{\max} is the maximum distance in the configuration space and \mathcal{V}_{\max} is the maximum speed of the agent at a free space, respectively. Note that the form (6) includes a dimensionless free parameter α that indirectly governs the safety distance. Fig. 4 shows the plots of the velocity function profiles at several values of α . The velocity map created from the binary map (Fig. 2), using the form (6) with $\alpha = 3$, is shown in Fig. 3.

Next, the second FMM is executed from the initial position \mathbf{x}_0 of the agent (or vehicle) to compute the time grid map $T(\mathbf{x})$, respecting the environmental constraints through $V(\mathbf{x})$. Finally, the path is obtained again by applying the gradient descent algorithm to $T(\mathbf{x})$ and the resulting path for the example case shown in Fig. 6.

The strength of the FMM-based method lies in its unparalleled computational speed when dealing with specific types of optimization problems. For instance, to provide a more intuitive grasp of the computational efficiency inherent in FMM-based methods, we delve into some practical specifics. The process of extracting a path from a grid of size 10^7 typically demands only a matter of seconds when employing a single-core machine. To put this into a simpler perspective, it is comparable to handling a two-dimensional pixel image measuring 4000×4000 in dimensions. It is also noteworthy that the application of the FMM across multiple iterations does not burden the optimization process with any substantial computational time constraints. The efficiency of the FMM-based method inspires the development of a new framework for various scenarios of modern operations of uncrewed vehicles in the subsequent section.

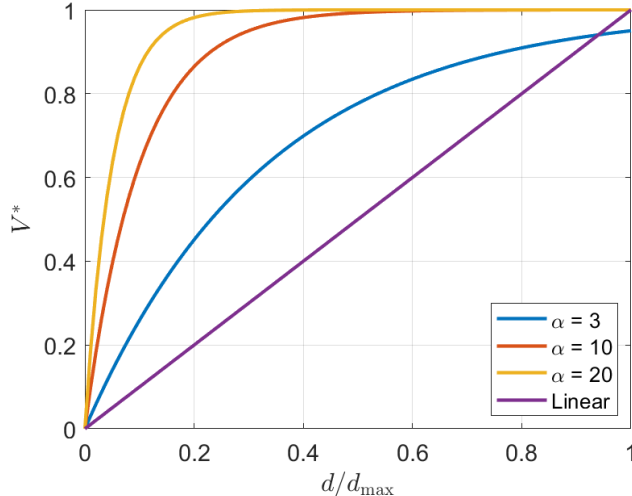


Figure 4: Plots of velocity functions (6) as a function of normalized distance d/d_{\max} for different values of α . The vertical axis $V^*(= V/V_{\max})$ is a normalized velocity by the maximum speed. In general, a smaller value of α results in a larger imposed safety distance.

3 FMM-based Rendezvous Path Planning for a Team of Heterogeneous Vehicles

The goal of this section is to introduce an innovative approach to leveraging the FMM-based method within a multi-agent path planning domain. In particular, we put forward an FMM-based rendezvous path planning algorithm designed for a diverse team of vehicles. The team is tasked with efficiently converging at a single location, aiming for optimal efficiency in pursuit of a general goal.

3.1 Problem Statement

This paper considers the problem of finding paths for $N(\geq 2)$ heterogeneous vehicles in a team, which are tasked with rendezvousing within a minimal time. The region of interest Ω is assumed to be represented by an occupancy grid map, where each pixel is either free $\mathcal{C}_{\text{free}}$ or occupied $\Omega \setminus \mathcal{C}_{\text{free}}$. According to the Ref. [34], a path is viewed as a continuous function $\tau : [0, 1] \rightarrow \mathcal{C}_{\text{free}}$, in which each point along the path is given by $\tau(s)$ for some $s \in [0, 1]$. Here, $\tau(0)$ corresponds to the starting point of the agent whereas $\tau(1)$ denotes the target point. Although the orientation of each vehicle will not be considered in this work, it is also feasible to incorporate their orientations using the existing methodology [30].

We assume that the starting position $\tau^i(0)$ of each vehicle in the team is given. Note that we introduced the index $i = 1, \dots, N$ to denote each vehicle. Then, the rendezvous path planning for the team is divided into two sub-problem. The first problem is to determine the optimal rendezvous point \mathbf{x}_m such that

$$\mathbf{x}_m = \arg \min_{\mathbf{x} \in \mathcal{C}_{\text{free}}} \mathcal{F}(\mathbf{x}), \quad (7)$$

where \mathcal{F} is a general cost function. The second sub-problem is to determine the optimal path $\tau^i(0)$ from initial point of each agent to the optimal point $\tau^i(1) = \mathbf{x}_m$.

From now on, for the purpose of illustration, we fix the optimizing function \mathcal{F} as the meeting time. In

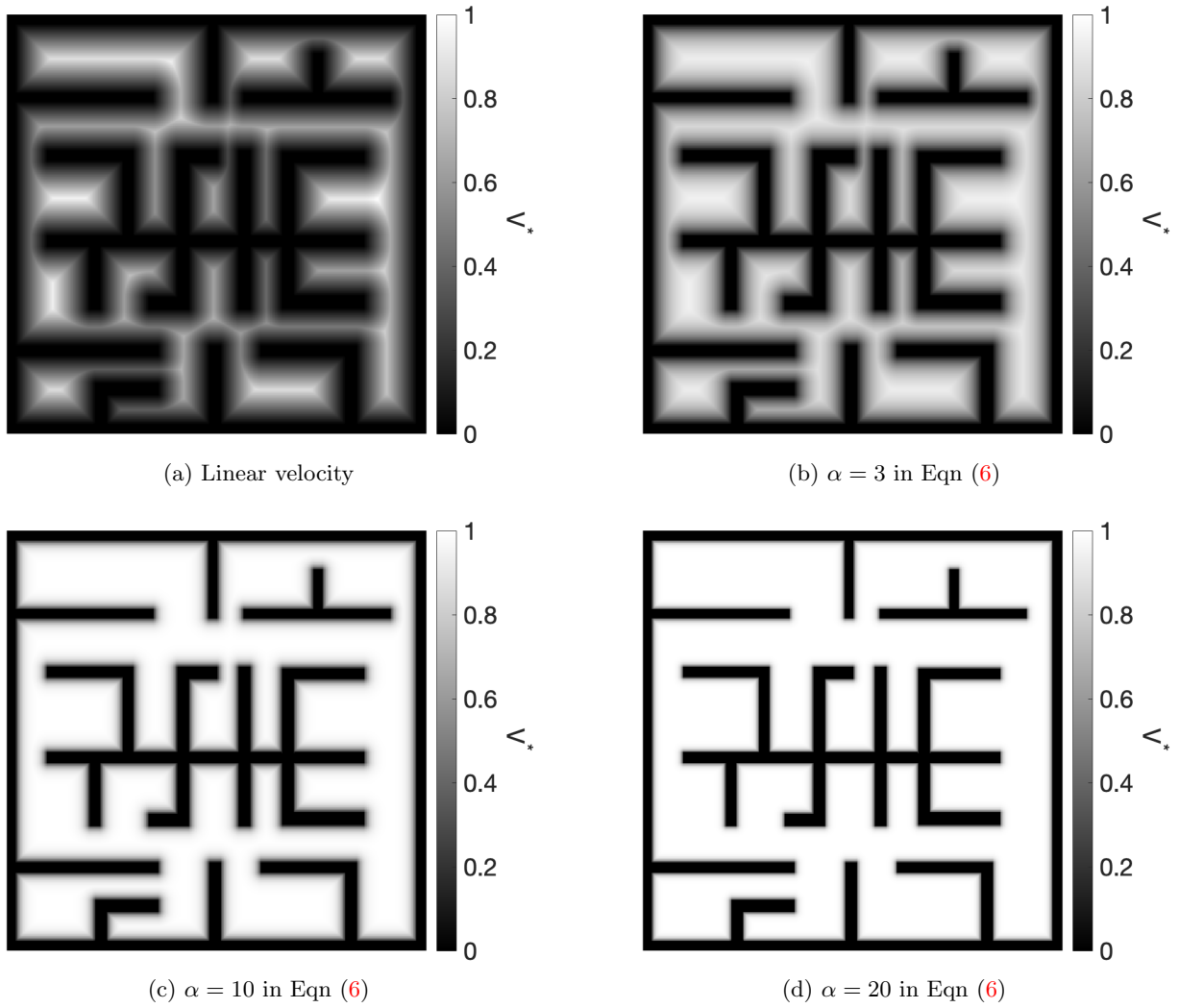


Figure 5: Comparison of velocity maps generated from the different velocity forms shown in Fig. 4. Sharper increase of V^* to value 1 results in a larger safety distance.

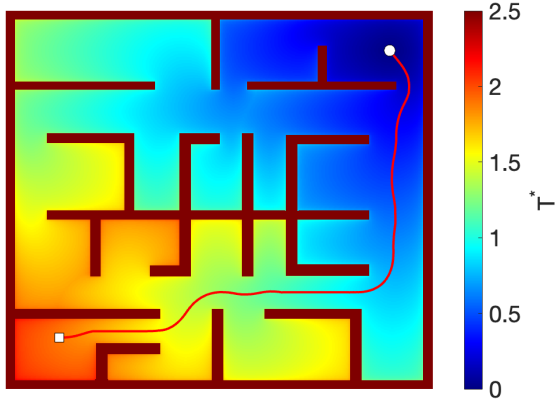


Figure 6: The optimized path after applying the gradient descent algorithm is plotted on the time grid. The white circle denotes the start point, while the square indicates the endpoint.

rendezvous tasks, this corresponds to the arrival time of last agent, which is written as

$$\mathcal{F}(\mathbf{x}) = \max [T^1(\mathbf{x}), T^2(\mathbf{x}), \dots, T^N(\mathbf{x})]. \quad (8)$$

where $T^i(\mathbf{x})$ denotes the arrival time for all $\mathbf{x} \in \mathcal{C}_{\text{free}}$, which will be also referred to as a time grid onwards.

3.2 The algorithm

Now, we describe our approach to the aforementioned rendezvous path planning problem. Considering the different initial position of each agent, a single implementation of the FMS method will yield $T^i(\mathbf{x})$ for all point in Ω . During this step, one can consider the arrival time $T^i(x)$ of each agent can be determined considering the different velocities and the safe distances imposed by environments. Once the arrival time maps for all agents are prepared, the best meeting point \mathbf{x}_m , which minimizes the cost $F(\mathbf{x})$ can be conveniently determined by

$$\mathbf{x}_m = \arg \min_{\mathbf{x} \in \mathcal{C}_{\text{free}}} (\max [(T^1(\mathbf{x}), T^2(\mathbf{x}), \dots, T^N(\mathbf{x}))]) \quad (9)$$

This approach can be easily generalized for situations where agents have different operation conditions, such as moving cost or fuel consumption rate, operation domain, or dynamics properties.

Below provides the implementation detail of the presented approach using an example of rendezvous planning for three agents, which are initially located at three different corners of a given binary occupancy map previously shown in Fig. 2. The initial positions are shown in Fig. 7a, Fig. 7b, and Fig. 7c. For simplicity, we assume that the vehicles are identical, which means that the vehicles travel with the same dynamics and at a same and constant speed. Specifically, $\alpha = 3$ and $\mathcal{V}_{\text{max}} = 1$ is used in the example.

The algorithm first begins by following the standard step of the FMS method to measure the distance to the distance $d \in \mathbb{R}^+$ to the nearest obstacles on every point in the grid. The first FMM runs from the initial surfaces of obstacles to fill up d -values on every non-occupied point in $\mathcal{C}_{\text{free}} \subset \Omega$, using the uniform velocity $V(\mathbf{x}) = 1$. Next, we generate a velocity map $V^i(\mathbf{x})$ for each agent $i \in \{1, 2, \dots, N\}$ using the velocity function (6). Each agent may have a different value of safety parameter α and the maximum allowable speed \mathcal{V}_{max} . The velocity map for the binary occupancy map using the the form is shown in Fig. 3.

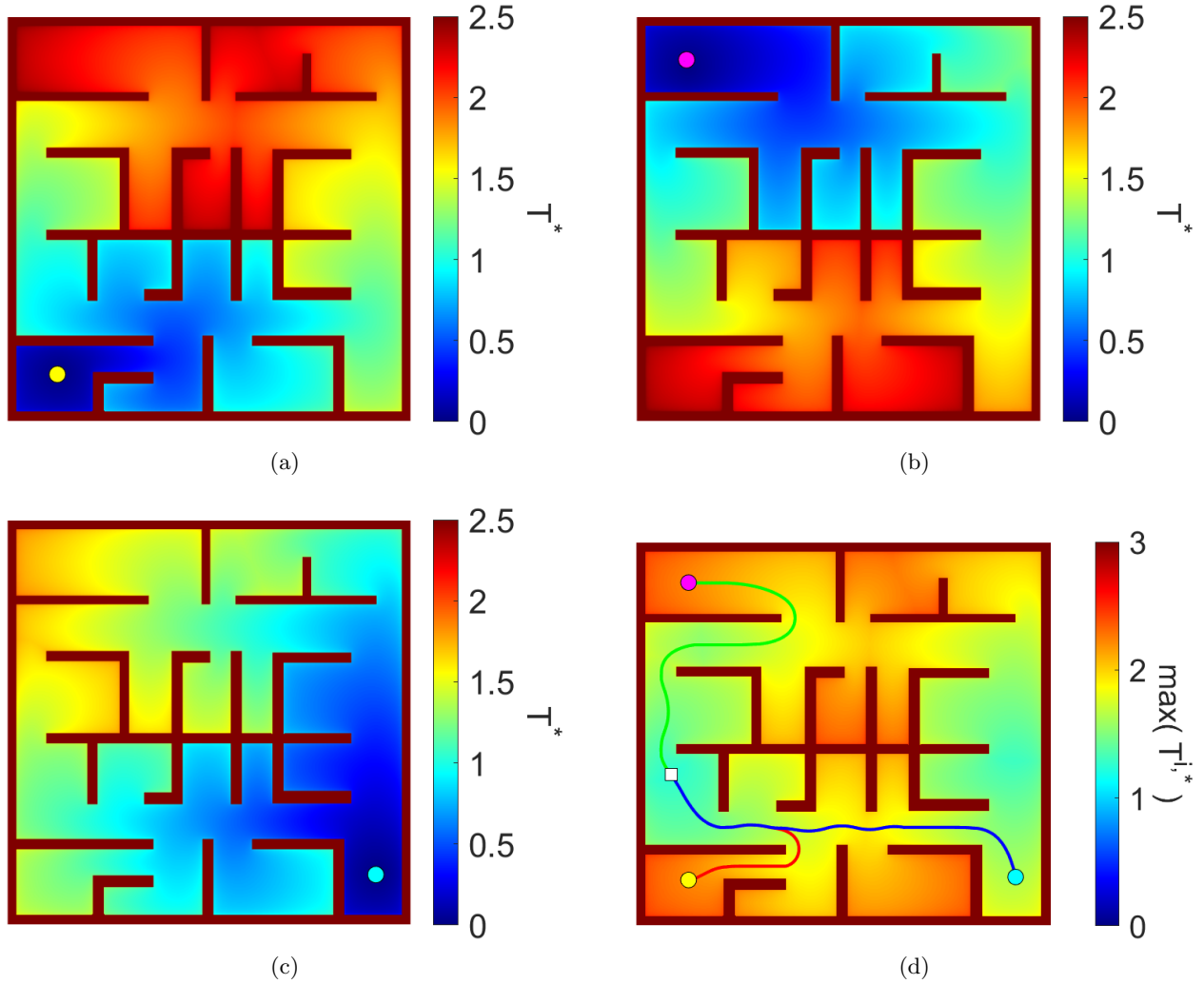


Figure 7: (a-c) The normalized arrival time T^* maps for three agents located at different initial points. (d) The optimized path drawn on $\mathcal{F}(\mathbf{x})$ as defined in the form (8).

Then, we run the second FMM multiple times starting from each initial position of agent \mathbf{x}_0^i , which corresponds to $\tau^i(0)$. This second round of FMM computation is executed to propagate a source wave point located at the target point until the arrival time T value at the initial point is determined. At each iteration, we obtain the arrival time of map $T^i(\mathbf{x})$ for each agent. Once the iterations of the second FMM finish, the optimal point \mathbf{x}_m can be determined directly from the form (9). The result of the term in (9), $\max [(T^1(\mathbf{x}), \dots, T^N(\mathbf{x}))]$, is shown with a color map in Fig. 7d.

Lastly, the optimized path τ^i for each agent to the rendezvous point is determined by applying the gradient descent algorithms to the time grid $T^i(\mathbf{x})$. This trajectory optimization step is inferred from the maximum gradient direction of $T(\mathbf{x})$. The final outcome of the FMS method is the optimized continuous path τ , a collection of point in Ω that guides trajectory of agents as shown in Fig. 6. The procedure is summarized in Algorithm 1.

Algorithm 1 FMM-based path optimization for multi-agent rendezvous

Input: A binary occupancy map $\Omega = \mathcal{C}_{\text{free}} \cup \mathcal{C}_{\text{free}}^c$, a cost function $\mathcal{F}(\mathbf{x})$, positions of obstacles \mathbf{x}_{obs} and initial points of total N agents $\tau^i(0) \in \Omega$

Output: The best point $\mathbf{x}_m \in \mathcal{C}_{\text{free}}$ that optimize the cost \mathcal{F} , and the optimized path τ^i for each agent

- 1: Execute the fast marching method from $\partial\mathcal{C}_{\text{free}}^c$ to compute the minimum distance $d(\mathbf{x})$ from obstacles
 - 2: **for** $i = 1$ to N **do**
 - 3: Calculate the maximum velocity field $V^i(\mathbf{x})$ using $d(\mathbf{x})$
 - 4: Execute the fast marching method from \mathbf{x}_0^i to compute $T^i(x)$
 - 5: **end for**
 - 6: Determine the optimizing point \mathbf{x}_m that minimizes $\mathcal{F}(\mathbf{x})$
 - 7: **for** $i = 1$ to N **do**
 - 8: Execute the fast marching method using $V^i(\mathbf{x})$ from \mathbf{x}_0^i to \mathbf{x}_{op}
 - 9: Use the maximum gradient descent algorithm to determine the path τ^i from \mathbf{x}_0^i to \mathbf{x}_{op} .
 - 10: **end for**
-

4 Experiment

In this section, we conduct a numerical experiment that showcases an application of the suggested method in more realistic cases. We consider a virtual scenario of rendezvous task for a team of heterogeneous vehicles. The experimental setting is as follows.

4.1 Experimental set up

First, we created a computational domain to simulate a realistic environment. We chose the Tampa Bay area as our test domain. We used a satellite image from NASA’s Earth Observatory (as shown in Fig. 8a)². Also, the GRIP tool (*Graphically Represented Image Processing engine*) [35] was employed to convert the satellite image into a binary configuration space map. The primary objective of image processing at this stage was to distinguish water bodies and land areas, as illustrated by white and black pixels respectively in Fig. 8b.

Next, we built a team of heterogeneous agents, of which member vehicles comprised four types: an uncrewed underwater vehicle (UUV), an uncrewed surface vehicle (USV), an uncrewed ground vehicle (UGV), and an uncrewed aerial vehicle (UAV). The UUV operates exclusively underwater but is limited by operational depth constraints. Consequently, UUV operations are required to take place at a considerable distance from the shoreline. On the other hand, the USV is designed for slower mobility, but it has the capability to navigate areas closer to the coastline. In contrast, the UGV’s operational domain is limited to land. Lastly, the UAV, being an aerial platform, is assumed to move at a constant speed without encountering any obstacles.

Operational constraints for the aforementioned heterogeneous agents were addressed using their respective velocity maps $V^i(\mathbf{x})$. The primary tools were the magnitude of the penalty parameter α in (6) and mirroring of binary image. To begin with, it is reasonable to impose a higher penalty to the operating velocity of UUV in the proximity to land, since UUV is required to operate at a far distance from the shoreline.

²<https://earthobservatory.nasa.gov/images/4745/tampa-bay-florida>

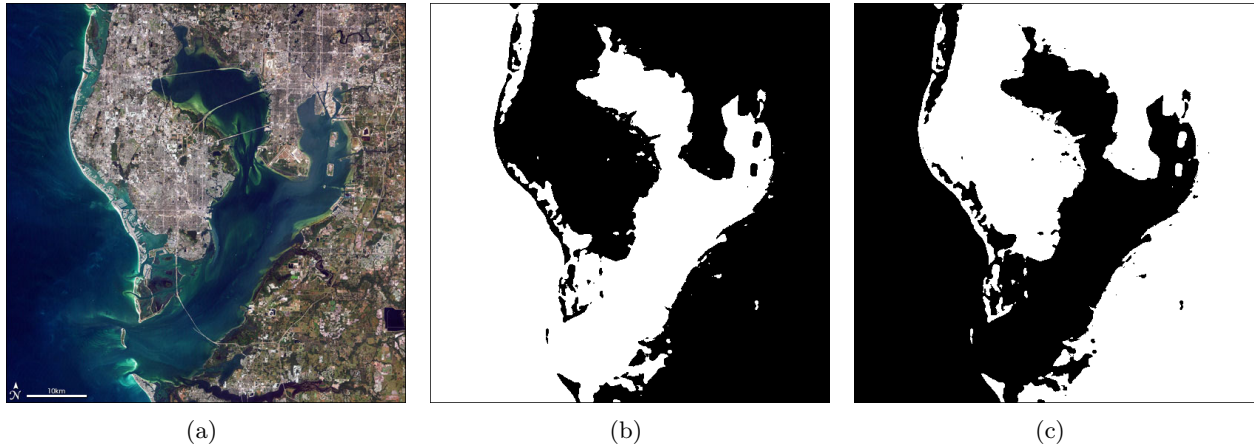


Figure 8: (a) Satellite image of Tampa Bay, FL. Downloaded from NASA Earth Observatory (b) Processed binary image from Fig. 8a for the USV and UUV; (c) Processed binary image for UGV, which is an inverse of Fig. 8b

Thus, we set the penalty parameter to $\alpha^{uu} = 100$, while the values of α^{us} , α^{ug} are set to 3. Moreover, in order to address the specific land travel limitation of the UGV, the operation domain of UGV was obtained by the mirroring of binary operational domain of ocean vehicles (i.e. USV, UUV), the result of which is shown in Fig. 8c. For UAVs traveling above both water and land, their domain was considered as free space without obstacles.

The remaining parameters are the maximum operational speed \mathcal{V}_{\max}^i of each vehicle. In actual applications, these parameters should reflect the actual performances of agents. In this virtual test, we assumed the following scenario to demonstrate the full potential of the present approach. First, the maximum operational speed of UGV was assumed to be the slowest among all agents, considering case where UGVs need to move as a group or encounter additional environmental restrictions (such as traffic or changes in topography). Then, we normalized velocities of vehicle using the maximum speed of UGV, and thus we write $\mathcal{V}_{\max}^{ugv} = 1$. The maximum speeds of USV and UUV were set to same $\mathcal{V}_{\max}^{uu} = \mathcal{V}_{\max}^{us} = 2$, and the UAV was assumed to have the highest navigation speed, and set to $\mathcal{V}_{\max}^{uav} = 3$.

With the prescribed setting, we applied the Algorithm 1 to solve the optimization problem of rendezvous path planning.

4.2 Results

We executed the first FMM (of the FMS) for each vehicle from arbitrarily selected initial points, as seen by the red dots in Fig. 9a-Fig. 9d. The computed time grid $T^i(\mathbf{x})$ for each vehicle is also visualized in the same plots. One distinguished case is Fig. 9d which shows unimpeded paths for the UAV throughout the environment.

Next, we note that an additional procedure that is not described in Algorithm 1 is necessary, as the UGV operates on the complementary domain of the UUV and USV in our test scenario. Note that candidates for the rendezvous point should be located on the shoreline, which belongs to the obstacles (i.e. $\Omega \setminus \mathcal{C}_{\text{free}}$) in the first FMM for any agent. To address such issue, we extended the time grid $T^i(\mathbf{x})$ to the edges of obstacles. Grid cells on the edge of binary images (Fig. 8b and Fig. 8c) were first detected using MATLAB’s “edge” function, and the $T^i(\mathbf{x})$ on edges were inferred from the minimum time value among the adjacent grid

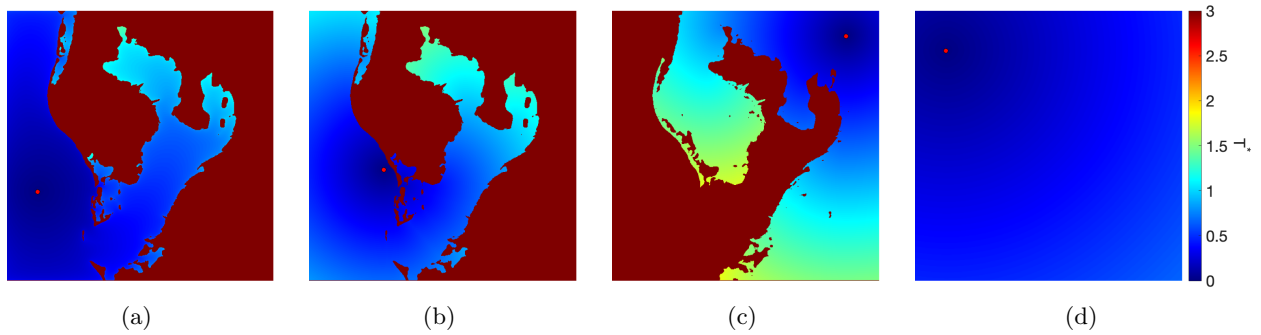


Figure 9: The time grids $T^i(\mathbf{x})$ of the (a) UUV, (b) USV, (c) UGV, and (d) UAV. The red dot in each plot denote the initial position of the vehicle.

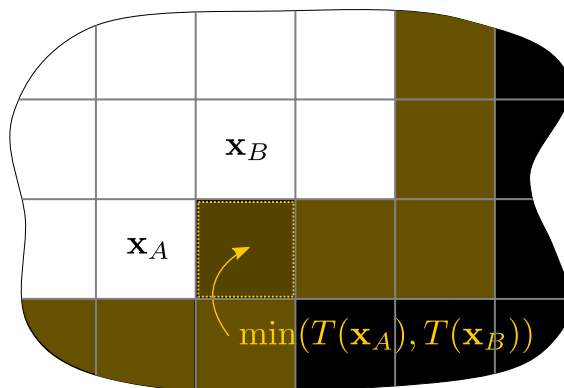


Figure 10: A mnemonic that outlines procedures for extending the time grid to accommodate situations where vehicles operate in non-intersecting domains, specifically the UUV/USV and UGV.

points. Fig. 10 illustrates this procedure. This results in a subset of the shoreline emerging as the candidate for the rendezvous point as seen in Fig. 11. Then, in the same figure, the black dot, which represents the optimal rendezvous point where all vehicles can converge in the minimum time, is determined by the form (9).

Next, the algorithm computes a path for each vehicle using the gradient descent method. Fig. 12a illustrates the UUV’s trajectory, characterized by significant turns to remain within its operational range, attributable to the low alpha value. On the contrary, Fig. 12b exemplifies the USV’s efficiency in navigating between islands. The UGV’s path in Fig. 12c remains confined to land, adhering to its intended operational domain. Lastly, the paths for all vehicles are summarized in Fig. 13, which also includes the simplest UAV’s path unhindered by obstacles due to its aerial capabilities.

Overall, we see that the resulting paths in Fig. 13 align well with the assumed operational constraints of the member vehicles, offering realistic planning outcomes. While the paths include overlaps between the USV and UGV, path conflicts are not an issue in the test scenario, since the agents have unique operational domains; they would not collide even if their paths overlap at the same time.

5 Discussion

In this section, we highlight the merits of our methodology in two ways.

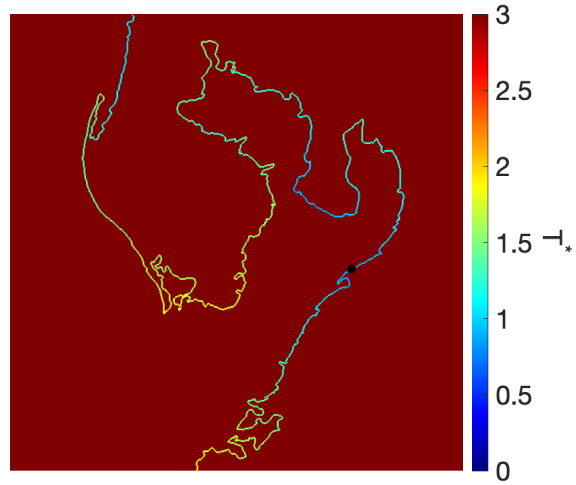


Figure 11: An extended time grid defined on shoreline to compute the rendezvous point \mathbf{x}_{op} , following the form (9).

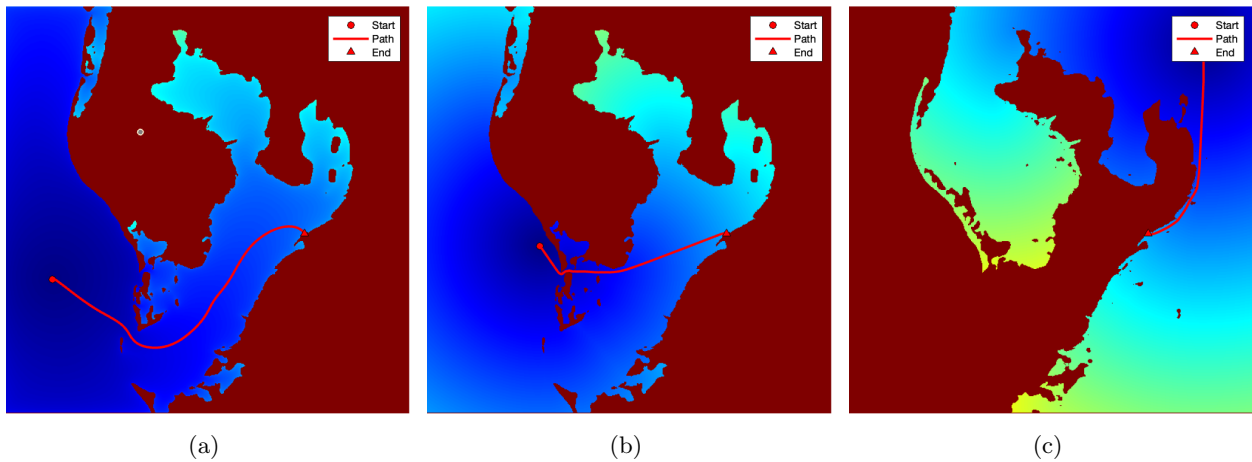


Figure 12: The paths planned for the (a) UUV, (b) USV, (c) UGV, shown over the each time grids Fig. 9.

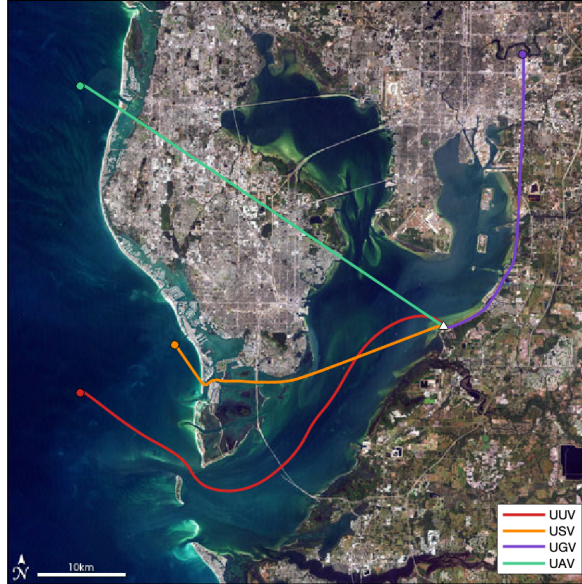


Figure 13: Path planning results plotted over the original satellite image. Circles denote starting points of vehicles, and the triangle denotes the computed optimal rendezvous point from the presented algorithm.

First, the authors are aware that constructing collision-free paths for agents is one of the most critical aspects of MAPF, even though our test scenario was free of such conflicts. However, even if agents share the same operational domain, under our framework it is easy to check whether overlapping paths will lead to collisions. This is because we have explicit information of each vehicle’s arrival time at overlapping points; path conflicts occurring at different times do not result in collisions between agents. We believe this is useful information for extending the current framework for truly collision-free path planning.

Lastly, we re-emphasize that the main contribution the present work is the formulation of the problem of multi-agent rendezvous task in the form of (8). While Algorithm 1 is straightforward under this formulation, a potential improvement can be found in the design of the velocity function (6) to respect a more detailed and realistic operational constraints of various types of vehicles.

Lastly, the main advantage of our approach is that the process is deterministic, implying that the resulting paths are guaranteed to be the globally optimized solution. In addition, the computational cost for determining paths of all agents is only proportional to the number of agent N . Therefore, at least for the rendezvous task as defined in (8), we claim that our approach outperforms heuristic, and stochastic, and machine learning based-method in terms of an unique solution approach and scalability.

6 Conclusion

Recent rapid advancements in uncrewed vehicle technology have significantly improved accessibility and cost-effectiveness, leading to their widespread integration across various domains, including ground, water, and air. As systems with uncrewed vehicles become ubiquitous, the demand for sophisticated navigation methodologies that can efficiently guide their interactions also becomes paramount. In this regard, the present work has introduced a new approach to path planning for multi-agent systems. Our method is rooted in the well-established framework of the FMM. The methodology presented in this paper leverages the capabilities of

the FMM to efficiently optimize trajectories for heterogeneous teams of agents, augmenting their operational efficiency and collective synergy.

To illustrate our approach, we considered an example path planning scenario involving four different types of uncrewed vehicles navigating around the Tampa Bay area. The results of virtual experiment demonstrated how the path planning task of a multi-agent system can benefit from the effectiveness of the FMM-based method, which conveniently incorporates the individual operational characteristics of the heterogeneous vehicles. The computational efficiency and flexibility of our approach open the door to various directions for future work.

- The optimization function \mathcal{F} can also be extended to incorporate various scenarios of rendezvous tasks other than the minimal time. For example, we plan to include different operational costs for heterogeneous vehicles to maximize the economic efficiency of rendezvous tasks.
- The proposed framework can be extended to path planning in presence of dynamic obstacles. This generalization will allow the algorithm to consider the collision between two different agents. The future work will investigate how the fast marching method can be modified in order to efficiently incorporate moving objects or other moving agents in the computation.
- Finally, we also envision extending our framework to different purposes of path planning for heterogeneous agents beyond rendezvous missions. This could involve group search optimization and assignment tasks.

Credit author statement

Jaekwang Kim: Conceptualization, Methodology, Software (original code development and numerical experiments), Validation, Writing. **Hyung-Jun Park:** Validation, Review. **Jaejeong Shin:** Conceptualization, Software (numerical experiments), Supervision, Writing.

Acknowledgements

Jaekwang Kim was supported by the Hongik University new faculty research support fund.

References

- [1] Jaejeong Shin et al. “Informative Multiview Planning for Underwater Sensors”. In: *IEEE Journal of Oceanic Engineering* 47.3 (2022), pp. 780–798. DOI: [10.1109/JOE.2021.3119150](https://doi.org/10.1109/JOE.2021.3119150).
- [2] Antonio L Diaz et al. “The Bathy-Drone: An autonomous uncrewed drone-tethered sonar system”. In: *Drones* 6.10 (2022), p. 294.
- [3] Fletcher Thompson and Damien Guihen. “Review of mission planning for autonomous marine vehicle fleets”. In: *Journal of Field Robotics* 36.2 (2019), pp. 333–354.
- [4] P. Melchior et al. “Consideration of obstacle danger level in path planning using A and Fast-Marching optimisation: comparative study”. In: *Signal Processing* 83.11 (2003). Fractional Signal Processing and Applications, pp. 2387–2396. ISSN: 0165-1684. DOI: [10.1016/S0165-1684\(03\)00191-9](https://doi.org/10.1016/S0165-1684(03)00191-9).

- [5] J. Yu and S. M. LaValle. “Structure and intractability of optimal multi-robot path planning on graphs”. In: *Proceedings of the AAAI Conference on Artificial Intelligence* 27 (2013), 1443–1449. DOI: [10.1609/aaai.v27i1.8541](https://doi.org/10.1609/aaai.v27i1.8541).
- [6] Q. Hu, W. Chen, and L. Guo. “Fixed-Time Maneuver Control of Spacecraft Autonomous Rendezvous With a Free-Tumbling Target”. In: *IEEE Transactions on Aerospace and Electronic Systems* 55 (2019), pp. 562–577. DOI: [10.1109/TAES.2018.2852439](https://doi.org/10.1109/TAES.2018.2852439).
- [7] S. R. Sahoo, R. N. Banavar, and A. Sinha. “Rendezvous in space with minimal sensing and coarse actuation”. In: *Automatica* 49 (2013), pp. 519–525. DOI: [10.1016/j.automatica.2012.11.024](https://doi.org/10.1016/j.automatica.2012.11.024).
- [8] V. Yordanova, H. Griffiths, and S. Hailes. “Rendezvous planning for multiple autonomous underwater vehicles using a Markov decision process”. In: *IET Radar, Sonar & Navigation* 11 (2017), pp. 1762–1769. DOI: [10.1049/iet-rsn.2017.0098](https://doi.org/10.1049/iet-rsn.2017.0098).
- [9] Rui Song, Yuanchang Liu, and Richard Bucknall. “A multi-layered fast marching method for unmanned surface vehicle path planning in a time-variant maritime environment”. In: *Ocean Engineering* 129 (2017), pp. 301–317. ISSN: 0029-8018. DOI: [10.1016/j.oceaneng.2016.11.009](https://doi.org/10.1016/j.oceaneng.2016.11.009).
- [10] Yuanchang Liu et al. “Predictive navigation of unmanned surface vehicles in a dynamic maritime environment when using the fast marching method”. In: *International Journal of Adaptive Control and Signal Processing* 31.4 (2017), pp. 464–488.
- [11] Xin ping Yan et al. “A novel path planning approach for smart cargo ships based on anisotropic fast marching”. In: *Expert Systems with Applications* 159 (2020), p. 113558. ISSN: 0957-4174. DOI: [10.1016/j.eswa.2020.113558](https://doi.org/10.1016/j.eswa.2020.113558).
- [12] Yadong Zhang et al. “A path planning method for the autonomous ship in restricted bridge area based on anisotropic fast marching algorithm”. In: *Ocean Engineering* 269 (2023), p. 113546. ISSN: 0029-8018. DOI: [10.1016/j.oceaneng.2022.113546](https://doi.org/10.1016/j.oceaneng.2022.113546).
- [13] Pengfei Chen et al. “Global path planning for autonomous ship: A hybrid approach of Fast Marching Square and velocity obstacles methods”. In: *Ocean Engineering* 214 (2020), p. 107793. ISSN: 0029-8018. DOI: [10.1016/j.oceaneng.2020.107793](https://doi.org/10.1016/j.oceaneng.2020.107793).
- [14] H-J Park, H-D Seo, and P-S Lee. “Direct imposition of the wall boundary condition for simulating free surface flows in SPH”. In: *Structural Engineering and Mechanics* 78 (2021), pp. 497–518. DOI: [10.12989/sem.2021.78.4.497](https://doi.org/10.12989/sem.2021.78.4.497).
- [15] Hyung-Jun Park and Hyun-Duk Seo. “A new SPH-FEM coupling method for fluid–structure interaction using segment-based interface treatment”. In: *Engineering with Computers* (2023). DOI: [10.1007/s00366-023-01856-1](https://doi.org/10.1007/s00366-023-01856-1).
- [16] A. M. Jokisaari et al. “Benchmark Problems for Numerical Implementations of Phase Field Models”. In: *Computational Materials Science* 126 (2017), pp. 139–151. DOI: [10.1016/j.commatsci.2016.09.022](https://doi.org/10.1016/j.commatsci.2016.09.022).

- [17] C. S. Peskin. “Flow patterns around heart valves: A numerical method”. In: *Journal of Computational Physics* 10 (1972), pp. 252–271. DOI: [10.1016/0021-9991\(72\)90065-4](https://doi.org/10.1016/0021-9991(72)90065-4).
- [18] Jaekwang Kim et al. “A crystal symmetry-invariant Kobayashi–Warren–Carter grain boundary model and its implementation using a thresholding algorithm”. In: *Computational Materials Science* 199 (2021), p. 110575. DOI: [10.1016/j.commatsci.2021.110575](https://doi.org/10.1016/j.commatsci.2021.110575).
- [19] A. Telea. “An image inpainting technique based on the fast marching method”. In: *Journal of Graphics Tools* 9 (2004), pp. 23–34. DOI: [10.1080/10867651.2004.10487596](https://doi.org/10.1080/10867651.2004.10487596).
- [20] N. Forcadel, C. L. Guyader, and C. Gout. “An image inpainting technique based on the fast marching method”. In: *Numerical Algorithms* 48 (2008), pp. 189–211. DOI: [10.1007/s11075-008-9183-x](https://doi.org/10.1007/s11075-008-9183-x).
- [21] A. Valero-Gomez, J. V. Gomez, and L. Moreno S. Garrido. “The Path to Efficiency: Fast Marching Method for Safer, More Efficient Mobile Robot Trajectories”. In: *IEEE Robotics & Automation Magazine* 20 (2013), pp. 110–120. DOI: [10.1109/MRA.2013.22483095](https://doi.org/10.1109/MRA.2013.22483095).
- [22] S. Garrido, L. Moreno, and D. Blanco. “Voronoi diagram and fast marching applied to path planning”. In: *Proceedings 2006 IEEE International Conference on Robotics and Automation*. 2006, pp. 3049–3054.
- [23] Alberto Valero-Gomez et al. “The Path to Efficiency: Fast Marching Method for Safer, More Efficient Mobile Robot Trajectories”. In: *IEEE Robotics & Automation Magazine* 20.4 (2013), pp. 111–120. DOI: [10.1109/MRA.2013.2248309](https://doi.org/10.1109/MRA.2013.2248309).
- [24] S. Garrido, M. Malfaz, and D. Blanco. “Application of the fast marching method for outdoor motion planning in robotics”. In: *Robotics and Autonomous Systems* 61 (2013), pp. 106–114. DOI: [10.1016/j.robot.2012.10.012](https://doi.org/10.1016/j.robot.2012.10.012).
- [25] D. Alvarez et al. “3D robot formations path planning with fast marching square”. In: *Journal of Intelligent & Robotic Systems* 80 (2015), pp. 507–523. DOI: [10.1007/s10846-015-0187-1](https://doi.org/10.1007/s10846-015-0187-1).
- [26] Javier V Gómez, Nikolaos Mavridis, and Santiago Garrido. “Fast marching solution for the social path planning problem”. In: *2014 IEEE international conference on robotics and automation (ICRA)*. IEEE. 2014, pp. 1871–1876.
- [27] J.N. Tsitsiklisl. “Efficient algorithms for globally optimal trajectories”. In: *IEEE Transactions on Automatic Control* 40 (1995), pp. 1528–1538. DOI: [10.1109/9.4126245](https://doi.org/10.1109/9.4126245).
- [28] J. A. Sethian. “The Path to Efficiency: Fast Marching Method for Safer, More Efficient Mobile Robot Trajectories”. In: *Proceedings of the National Academy of Sciences of the United States of America* 93 (1996), pp. 1591–1595.
- [29] R. Sedgewick and K. Wayne. *Algorithms*. Addison-Wesley, 2008.
- [30] Yuanchang Liu and Richard Bucknall. “The angle guidance path planning algorithms for unmanned surface vehicle formations by using the fast marching method”. In: *Applied Ocean Research* 59 (2016), pp. 327–344. ISSN: 0141-1187. DOI: [10.1016/j.apor.2016.06.013](https://doi.org/10.1016/j.apor.2016.06.013).

- [31] Guoge Tan et al. “Fast marching square method based intelligent navigation of the unmanned surface vehicle swarm in restricted waters”. In: *Applied Ocean Research* 95 (2020), p. 102018. ISSN: 0141-1187. DOI: [10.1016/j.apor.2019.102018](https://doi.org/10.1016/j.apor.2019.102018).
- [32] Guoge Tan et al. “Adaptive adjustable fast marching square method based path planning for the swarm of heterogeneous unmanned surface vehicles (USVs)”. In: *Ocean Engineering* 268 (2023), p. 113432. ISSN: 0029-8018. DOI: [10.1016/j.oceaneng.2022.113432](https://doi.org/10.1016/j.oceaneng.2022.113432).
- [33] S. Garrido et al. “FM2: A Real-Time Sensor-Based Feedback Controller For Mobile Robots”. In: *International Journal of Robotics and Automation* 24 (2009), pp. 3169–3192. DOI: [10.2316/Journal.206.2009.1.206-3169](https://doi.org/10.2316/Journal.206.2009.1.206-3169).
- [34] Steven M LaValle. *Planning algorithms*. Cambridge university press, 2006.
- [35] Jonathan L Leitschuh and Thomas John Clark. *GRIP: Graphically Represented Image Processing engine*. Tech. rep. 100 Institute Road, Worcester MA 01609-2280 USA: Worcester Polytechnic Institute, 2016.